Trajectory Tracking by TP Model Transformation: Case Study of a Benchmark Problem

Zoltán Petres, *Student Member, IEEE*, Péter Baranyi, *Member, IEEE*, Péter Korondi, *Member, IEEE*, and Hideki Hashimoto, *Fellow, IEEE*

***Abstract*—The main objective of this paper is to study the recently proposed tensor-product-distributed-compensation (TPDC)-based control design framework in the case of tracking control design of a benchmark problem. The TPDC is a combination of the tensor product model transformation and the parallel distributed compensation framework. In this paper, we investigate the effectiveness of the TPDC design. We study how it can be uniformly and readily executed without analytical derivations. We show that the TPDC is straightforward and numerically tractable, and is capable of guarantying various different control performances via linear matrix inequality (LMI) conditions. All these features are studied via the state feedback trajectory control design of the translational oscillations with an eccentric rotational proof mass actuator system. The trajectory tracking capability for various tracking commands is optimized here by decay rate LMI conditions. Constraints on the output and control of the closed-loop system are also considered by LMI conditions. We present numerical simulations of the resulting closed-loop system to validate the control design.**

***Index Terms*—Linear matrix inequalities (LMIs), parallel distributed compensation (PDC), tensor product (TP) model transformation, trajectory command tracking, translational oscillations with an eccentric rotational proof mass actuator (TORA).**

NOMENCLATURE

- M Mass of cart.
- k Linear spring stiffness.
- m Mass of the proof mass actuator.
- I Moment of inertia of the proof mass actuator.
- e Distance between the rotation point and the center of the proof mass.
- N Control torque applied to the proof mass.
- q Translational position of the cart.
- θ Angular position of the rotational proof mass.

Manuscript received October 25, 2005; revised April 12, 2006. This work was supported in part by the Hungarian Scientific Research Fund (OTKA) under Grant F 049838 and Grant K 62836, and in part by the János Bolyai Postdoctoral Scholarship of the Hungarian Academy of Sciences.

Z. Petres is with the Computer and Automation Research Institute, Hungarian Academy of Sciences, 1111 Budapest, Hungary (e-mail: petres@tmit.bme.hu).

P. Baranyi is with the Computer and Automation Research Institute, Hungarian Academy of Sciences, 1111 Budapest, Hungary, and also with the Integrated Intelligent Systems Japanese–Hungarian Laboratory, Budapest University of Technology and Economics, 1111 Budapest, Hungary (e-mail: baranyi@sztaki.hu).

P. Korondi is with Budapest University of Technology and Economics, 1111 Budapest, Hungary.

H. Hashimoto is with the Institute of Industrial Science, The University of Tokyo, Tokyo 153-8505, Japan (e-mail: hashimoto@iis.u-tokyo.ac.jp).

Color versions of one or more of the figures in this paper are available online at http://ieeexplore.ieee.org.

Digital Object Identifier 10.1109/TIE.2007.894697

I. INTRODUCTION

THE tensor product (TP) model form is a dynamic model representation whereupon linear matrix inequality (LMI)-based control design techniques [1]–[5] can immediately be executed. It describes a class of linear-parameter-varying (LPV) models by the convex combination of linear time invariant (LTI) models, where the convex combination is defined by the weighting functions of each parameter separately. An important advantage of the TP model forms is that the convex hull of the given dynamic LPV model can readily be determined and analyzed in the TP model representation. Furthermore, the feasibility of the LMIs can be considerably relaxed in this representation via modifying the convex hull of the LPV model.

The TP model transformation is a recently proposed numerical method to transform LPV models into TP model form [6]–[8]. It is capable of transforming different LPV model representations (such as physical model given by analytic equations, fuzzy, neural network, genetic algorithm based models) into TP model form in a uniform way. In this sense it replaces the analytical derivations and affine decompositions (that could be a very complex or even an unsolvable task), and automatically results in the TP model form. Execution of the TP model transformation takes a few minutes by a regular Personal Computer. The TP model transformation minimizes the number of the LTI components of the resulting TP model. Furthermore, the TP model transformation is capable of resulting different convex hulls of the given LPV model.

One can find a number of LMIs under the parallel distributed compensation (PDC) framework that can immediately be applied to the TP model according to various control design specifications. Therefore, it is worth linking the TP model transformation and the PDC design framework [9].

In this paper, we revisit the multicriteria nonlinear control problem of the translational oscillations with an eccentric rotational proof mass actuator (TORA) system and derive controllers to track the general type of trajectory commands. We derive a controller that is capable of asymptotically converging to the command signal. The design also considers constraints on the control and output values. To optimize the tracking performance under the given constraints, we execute decay rate controller design.

The remainder of this paper is organized as follows. Section II introduces the tensor product distributed compensation (TPDC)-based controller design framework. Section III first describes the TORA system and discusses the goals and specifications of the controller. Then, the convex polytopic

model is given, and through several simulations, the designed controllers are analyzed. Finally, Section IV concludes the paper with the results.

II. TPDC

Consider the following LPV state-space model:

$$\begin{aligned}\dot{\mathbf{x}}(t) &= \mathbf{A}\left(\mathbf{p}(t)\right)\mathbf{x}(t) + \mathbf{B}\left(\mathbf{p}(t)\right)\mathbf{u}(t)\\ \mathbf{y}(t) &= \mathbf{C}\left(\mathbf{p}(t)\right)\mathbf{x}(t) + \mathbf{D}\left(\mathbf{p}(t)\right)\mathbf{u}(t)\end{aligned} \tag{1}$$

with input $\mathbf{u}(t) \in \mathbb{R}^k$, output $\mathbf{y}(t) \in \mathbb{R}^l$, and state vector $\mathbf{x}(t) \in \mathbb{R}^m$. The system matrix

$$\mathbf{S}\left(\mathbf{p}(t)\right) = \begin{pmatrix}\mathbf{A}\left(\mathbf{p}(t)\right) & \mathbf{B}\left(\mathbf{p}(t)\right)\\ \mathbf{C}\left(\mathbf{p}(t)\right) & \mathbf{D}\left(\mathbf{p}(t)\right)\end{pmatrix} \in \mathbb{R}^{(m+k)\times(m+l)} \tag{2}$$

is a parameter-varying object, where $\mathbf{p}(t) \in \Omega$ is a time-varying N-dimensional parameter vector and is an element of the closed hypercube $\Omega = [a_1, b_1] \times [a_2, b_2] \times \cdots \times [a_N, b_N] \subset \mathbb{R}^N$. Parameter $\mathbf{p}(t)$ can also include some elements of $\mathbf{x}(t)$. Therefore, this type of model is considered to belong to the class of nonlinear models.

The TP model transformation starts with the given LPV model (1) and results in the TP model representation

$$\dot{x} \approx \mathcal{S} \overset{N}{\underset{n=1}{\otimes}} \mathbf{w}_n(p_n)\begin{pmatrix}x\\ u\end{pmatrix} \tag{3}$$

which can always be transformed to the typical form

$$\begin{pmatrix}\dot{\mathbf{x}}(t)\\ \mathbf{y}(t)\end{pmatrix} \approx \sum_{r=1}^{R} w_r\left(\mathbf{p}(t)\right)\mathbf{S}_r\begin{pmatrix}\mathbf{x}(t)\\ \mathbf{u}(t)\end{pmatrix} \tag{4}$$

where

$$\left\|\mathbf{S}\left(\mathbf{p}(t)\right) - \sum_{r=1}^{R} w_r\left(\mathbf{p}(t)\right)\mathbf{S}_r\right\| \le \varepsilon.$$

Here, ε symbolizes the approximation error, and $w_r(\mathbf{p}(t) \in [0,1]$ are the coefficient functions. Let the size of $\mathbf{S}_r$ be $\mathbb{R}^{(m+k)\times(m+l)}$ in the following. The convex combination of the LTI vertex systems is ensured by the following conditions.

Definition 1: The model (4) is convex if

$$\forall r \in [1, R], \quad \mathbf{p}(t) \quad : \quad w_r\left(\mathbf{p}(t)\right) \in [0,1] \tag{5}$$

$$\forall \mathbf{p}(t) \quad : \quad \sum_{r=1}^{R} w_r\left(\mathbf{p}(t)\right) = 1. \tag{6}$$

This simply means that $\mathbf{S}(\mathbf{p}(t))$ is within the convex hull of the LTI vertex systems $\mathbf{S}_r$ for any $\mathbf{p}(t) \in \Omega$.

The matrix $\mathbf{S}(\mathbf{p}(t))$ has a finite-element TP model representation in many cases [$\varepsilon = 0$ in (4)]. In this case, we say that the TP model is exact.

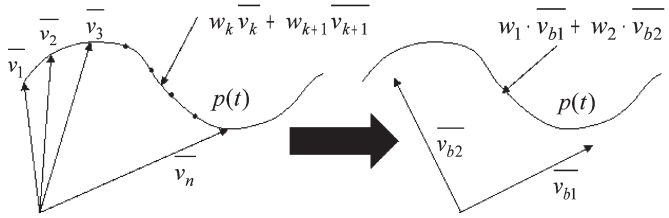

Fig. 1. Basic idea of TP model transformation.

The TP model transformation finds the minimal number of LTI systems in exact case. If the finite-element TP model does not exist, then the TP model transformation helps the tradeoff between the number of LTI vertex systems and the ε [7]. The basic idea is illustrated in Fig. 1 for case of $N = 1$.

The $\mathbf{p}(t)$ is sampled in n points by vectors $\bar{v}_k$. Between the discretized points, $\mathbf{p}(t)$ is approximated by interpolation. It is clear in this simple case that $\mathbf{p}(t)$ can be described by two orthogonal base vectors $\bar{v}_{b1}$ and $\bar{v}_{b2}$ in a properly selected coordinate system. This simple idea is generalized for TP transformation.

In the first step, the transformation generates a discrete finite-element TP model form from the system that can be described by analytical formulas, soft-computing models, or real-world measurement data. For analytical and soft-computing models, it is performed by numerical discretization over a hyper-rectangular grid, while for measurement data, the measurement process is designed to directly result in the discrete finite-element TP model. The system is known in discrete points, and an interpolation technique is necessary between the discrete points.

The next step is the selection of the base vectors in Fig. 1 and the selection of $\mathbf{S}_r$ in general case by high-order singular-value decomposition (HOSVD).

It is known from matrix algebra that each matrix can be written in the form

$$\mathbf{A} = \mathbf{U}\mathbf{S}\mathbf{V}^T \tag{7}$$

where $\mathbf{A}$ is an arbitrary $n \times m$ matrix, $\mathbf{U}$ is a matrix that contains the singular vectors of the matrix $\mathbf{A}\mathbf{A}^T$, and $\mathbf{S}$ contains the so-called singular values in its diagonal. $\mathbf{V}$ contains the singular vectors of the matrix $\mathbf{A}\mathbf{A}^T$ again. $\mathbf{S}$ is a diagonal matrix that is often denoted as a vector. The occurrence of zeros in matrix $\mathbf{S}$ allows us to decrease the size of matrix $\mathbf{A}$. In case of a tensor, it has to be unfolded into bidimensional space to form an ordinary matrix (first step in Fig. 2), and then the singular-value decomposition can be applied. The lines and columns are removed, which are multiplied by 0 in $\mathbf{S}$, thus obtaining a simplified system. Finally, the matrix must be packed back into its original tensor form. The above operations can be performed along every dimension, which ensures the best possible reduction of the system, which finally results in an HOSVD.

For further details about the TP model transformation, we refer to [7], [8], and [10]. There is a MATLAB Toolbox for TP model transformation. The toolbox is available

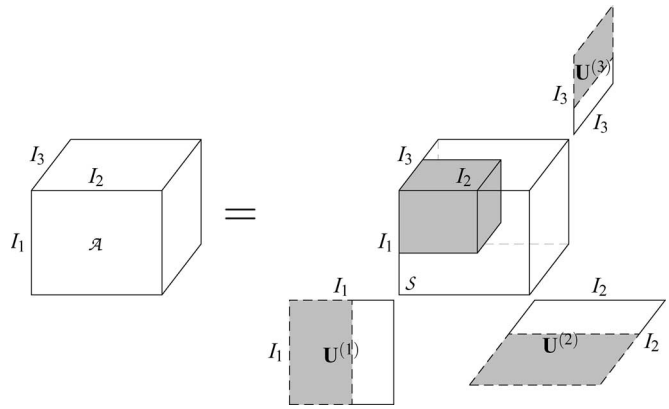

Fig. 2. HOSVD.

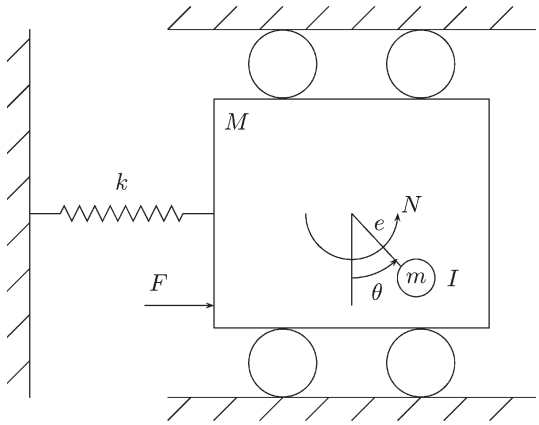

Fig. 3. TORA system.

for download together with documentation and examples at http://www.sztaki.hu/tpdc. The TP model transformation offers options to generate different types of weighting functions $w(\cdot)$. Different weighting functions determine different types of convex hulls of the given LPV model. For instance, in the case of generating tight convex, the TP model transformation results in LTI systems, whereas many of the LTI systems as possible are equal to $\mathbf{S}(\mathbf{p}(t))$ over some $\mathbf{p}(t) \in \Omega$, and the rest of the LTIs are close to $\mathbf{S}(\mathbf{p}(t))$ (in the sense of the L_2 norm). We generate this type of convex hull in the control design of this paper, as can be seen.

As an alternative way of LMI-based control design, the PDC framework was introduced by Tanaka and Wang [9]. The PDC design framework determines one LTI feedback gain to each LTI vertex system of a given TP model. The framework starts with the LTI vertex systems $\mathbf{S}_r$ and results in the vertex LTI gains $\mathbf{F}_r$ of the controller. These gains $\mathbf{F}_r$ are computed by the LMI-based stability theorems. After having $\mathbf{F}_r$, the control value $\mathbf{u}(t)$ is determined by the help of the same TP model structure as used in (4), i.e.,

$$\mathbf{u}(t) = -\left(\sum_{r=1}^{R} w_r\left(\mathbf{p}(t)\right)\mathbf{F}_r\right)\mathbf{x}(t). \tag{8}$$

The LMI theorems, which are to be solved under the PDC framework, are selected according to the stability criteria and the desired control performance. For instance, the speed of response and the constraints on the state vector or on the control value can be considered via properly selected LMI-based stability theorems.

III. Case Study of the TPDC

The study is conducted through a state feedback control design for the TORA system, which was originally studied as a simplified model of a dual-spin spacecraft with mass imbalance to investigate the resonance capture phenomenon [11], [12]. The same plant was later studied involving the rotational proof mass actuator for feedback stabilization of translational motion [13], [14]. The TORA system is also considered as a fourth-order benchmark problem [15]–[17]. The *International Journal of Robust and Nonlinear Control* published a series of studies about the control issue of the TORA system in Volume 8 in 1998 [18].

A. Equations of Motion

The TORA system is shown in Fig. 3 with the notation defined above. The oscillation consists of a cart of mass M connected to a fixed wall by a linear spring of stiffness k. The cart is constrained to have 1-D travel in the horizontal plane. The rotating proof mass actuator is attached to the cart. The control torque is applied to the proof mass. $\theta = 0^\circ$ is perpendicular to the motion of the cart, while $\theta = 90^\circ$ is aligned with the positive q direction. The equations of motion are given by [18]

$$(M+m)\ddot{q} + kq = -me(\ddot{\theta}\cos\theta - \dot{\theta}^2\sin\theta) \tag{9}$$

$$(I+me^2)\ddot{\theta} = -me\ddot{q}\cos\theta + N \tag{10}$$

with normalization [13]

$$\xi \simeq \sqrt{\frac{M+m}{I+me^2}}q \quad \tau \simeq \sqrt{\frac{k}{M+m}}t \tag{11}$$

$$u \simeq \frac{M+m}{k(I+me^2)}N \tag{12}$$

and the equations of motion become

$$\ddot{\xi} + \xi = \rho(\dot{\theta}^2\sin\theta - \ddot{\theta}\cos\theta) \tag{13}$$

$$\ddot{\theta} = -\rho\ddot{\xi}\cos\theta + u \tag{14}$$

where ξ is the normalized cart position, and u is the nondimensional control torque. τ is the normalized time whereupon the differentiation is understood. ρ is the coupling between the rotational and translational motions, i.e.,

$$\rho \simeq \frac{me}{\sqrt{(I+me^2)(M+m)}}. \tag{15}$$

The above equations can be given in the state-space model form

$$\begin{aligned}\dot{x} &= f(x) + g(x)u \\ y &= c(x)\end{aligned} \tag{16}$$

where

$$f(x) = \begin{pmatrix} x_2 \\ \frac{-x_1+\rho x_4^2 \sin x_3}{1-\rho^2 \cos^2 x_3} \\ x_4 \\ \frac{\rho \cos x_3 \left(x_1-\rho x_4^2 \sin x_3\right)}{1-\rho^2 \cos^2 x_3} \end{pmatrix}$$

$$g(x) = \begin{pmatrix} 0 \\ \frac{-\rho \cos x_3}{1-\rho^2 \cos^2 x_3} \\ 0 \\ \frac{1}{1-\rho^2 \cos^2 x_3} \end{pmatrix}$$

$$c(x) = \begin{pmatrix} x_1 & 0 & 0 & 0 \\ 0 & 0 & x_3 & 0 \end{pmatrix} \tag{17}$$

and $x = (x_1\ x_2\ x_3\ x_4)^T = (\xi\ \dot{\xi}\ \theta\ \dot{\theta})^T$. Let us write the above equation in the typical form of LPV state-space model as

$$\dot{x} = \mathbf{S}(p)\begin{pmatrix} x \\ u \end{pmatrix} \quad y = \mathbf{C}x \tag{18}$$

where system matrix $\mathbf{S}(p)$ contains

$$\mathbf{S}(p) = (\mathbf{A}(p) \quad \mathbf{B}(p))$$

and $p = (x_3\ x_4) \in \Omega$ is a time-varying 2-D parameter vector, so as

$$\mathbf{A}(x_3, x_4) = \begin{pmatrix} 0 & 1 & 0 & 0 \\ -\frac{1}{1-\rho^2 \cos^2 x_3} & 0 & 0 & \frac{\rho x_4 \sin x_3}{1-\rho^2 \cos^2 x_3} \\ 0 & 0 & 0 & 1 \\ \frac{\rho \cos x_3}{1-\rho^2 \cos^2 x_3} & 0 & 0 & \frac{-x_4 \rho^2 \cos x_3 \sin x_3)}{1-\rho^2 \cos^2 x_3} \end{pmatrix}$$

$$\mathbf{B}(x_3) = g(x)$$

$$\mathbf{C} = \begin{pmatrix} 1 & 0 & 0 & 0 \\ 0 & 0 & 1 & 0 \end{pmatrix}. \tag{19}$$

The laboratory version of the TORA system is described in [16]. The nominal configuration of this version is given in Table I.

B. Control Specifications

We extend the design specifications detailed in [18, p. 309] and [19]–[21] of the benchmark problem of the TORA system for tracking control.

TABLE I
PARAMETERS OF THE TORA SYSTEM

Description	Parameter	Value	Units
Cart mass	M	1.3608	kg
Arm mass	m	0.096	kg
Arm eccentricity	e	0.0592	m
Arm inertia	I	0.0002175	kg m^2
Spring stiffness	k	186.3	N/m
Coupling parameter	ρ	0.200	—

Design a tracking controller that satisfies the following criteria.

- The trajectory command in unknown.
- The type of the trajectory may vary during control.
- The closed-loop system asymptotically converges to trajectory command and is stable.
- The physical configuration of the system necessities the constraint $|q| \leq 0.025$ m.
- During trajectory tracking, the control value is limited by $N \leq 0.100$ N $\cdot$ m, although somewhat higher torques can be tolerated for short periods.

If we have no information about the trajectory in the design phase, and we assume that it can even vary from one type to other type during the control, then we cannot specify our design for any expected trajectory. Therefore, our goal is to design a controller with a good speed of response (decay rate control), and thus, we expect that it is capable of acting for fast varying command signals as well.

C. Finite-Element TP Model of the TORA System

We execute the TP model transformation on the LPV model (18) of the TORA. As a first step of the TP model transformation, we have to define the transformation space Ω. If we see the simulations in the papers of the special issue [18]–[21], we find that θ is always smaller than 0.85 rad, and according to the maximum allowed torque $u = 0.1$ N, the system would not achieve larger $\dot{\theta}$ than 0.5 rad but could have a little overshoot, see [18, p. 392] and Section III-C of this paper. Therefore, we define the transformation space as $\Omega = [-a, a] \times [-a, a]$ $(x_3(t) \in [-a, a]$ and $x_4(t) \in [-a, a])$, where $a = 45/180\ \pi$ rad (note that these intervals can be arbitrarily defined). The TP model transformation starts with the discretization over a rectangular grid. Let the density of the discretization grid be 101 $\times$ 101 on $(x_3(t) \in [-a, a]) \times (x_4(t) \in [-a, a])$. The result of the TP model transformation shows that the TORA system can be exactly given as the combination of ten LTI systems

$$\mathbf{S}(p) = \sum_{r=1}^{10} w_r(x_3, x_4)(\mathbf{A}_r x + \mathbf{B}_r u). \tag{20}$$

The weighting functions $w_r(\cdot)$ of the polytopic model are presented in Fig. 4.

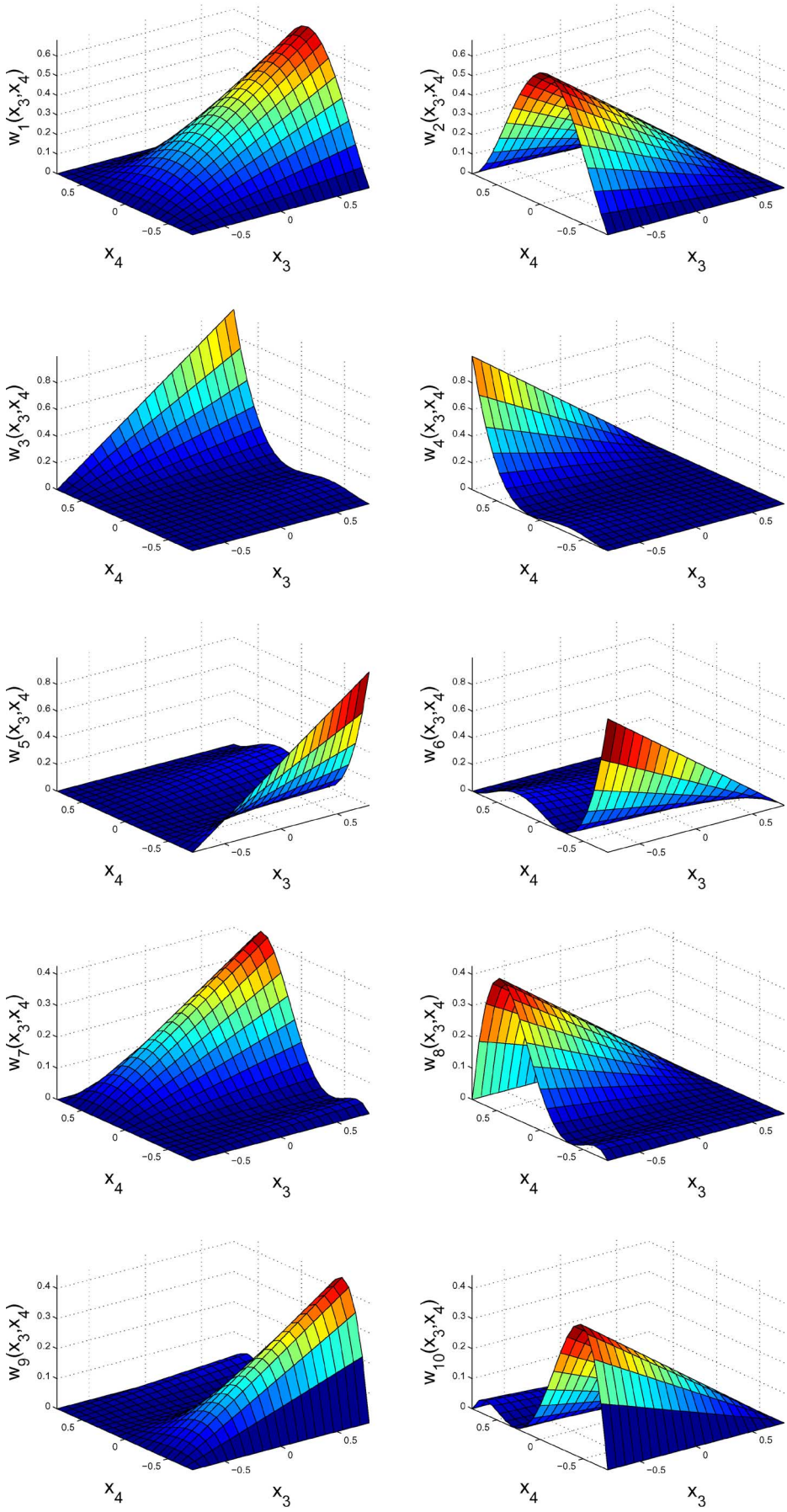

Fig. 4. Weighting functions of the polytopic model 2.

The LTI system matrices of the polytopic model are

$$\mathbf{A}_1 = \begin{pmatrix} 0 & 1.0000 & 0 & 0 \\ -1.0493 & 0 & 0 & 0.0094 \\ 0 & 0 & 0 & 1.0000 \\ 0.2288 & 0 & 0 & -0.0010 \end{pmatrix}$$

$$\mathbf{B}_1 = \begin{pmatrix} 0 \\ -0.2288 \\ 0 \\ 1.0493 \end{pmatrix}$$

$$\mathbf{A}_2 = \begin{pmatrix} 0 & 1.0000 & 0 & 0 \\ -1.0493 & 0 & 0 & -0.0094 \\ 0 & 0 & 0 & 1.0000 \\ 0.2288 & 0 & 0 & 0.0010 \end{pmatrix}$$

$$\mathbf{B}_2 = \begin{pmatrix} 0 \\ -0.2288 \\ 0 \\ 1.0493 \end{pmatrix}$$

$$\mathbf{A}_3 = \begin{pmatrix} 0 & 1.0000 & 0 & 0 \\ -1.0204 & 0 & 0 & 0.1133 \\ 0 & 0 & 0 & 1.0000 \\ 0.1443 & 0 & 0 & -0.0160 \end{pmatrix}$$

$$\mathbf{B}_3 = \begin{pmatrix} 0 \\ -0.1443 \\ 0 \\ 1.0204 \end{pmatrix}$$

$$\mathbf{A}_4 = \begin{pmatrix} 0 & 1.0000 & 0 & 0 \\ -1.0204 & 0 & 0 & -0.1133 \\ 0 & 0 & 0 & 1.0000 \\ 0.1443 & 0 & 0 & 0.0160 \end{pmatrix}$$

$$\mathbf{B}_4 = \begin{pmatrix} 0 \\ -0.1443 \\ 0 \\ 1.0204 \end{pmatrix}$$

$$\mathbf{A}_5 = \begin{pmatrix} 0 & 1.0000 & 0 & 0 \\ -1.0204 & 0 & 0 & -0.1133 \\ 0 & 0 & 0 & 1.0000 \\ 0.1443 & 0 & 0 & 0.0160 \end{pmatrix}$$

$$\mathbf{B}_5 = \begin{pmatrix} 0 \\ -0.1443 \\ 0 \\ 1.0204 \end{pmatrix}$$

$$\mathbf{A}_6 = \begin{pmatrix} 0 & 1.0000 & 0 & 0 \\ -1.0204 & 0 & 0 & 0.1133 \\ 0 & 0 & 0 & 1.0000 \\ 0.1443 & 0 & 0 & -0.0160 \end{pmatrix}$$

$$\mathbf{B}_6 = \begin{pmatrix} 0 \\ -0.1443 \\ 0 \\ 1.0204 \end{pmatrix}$$

$$\mathbf{A}_7 = \begin{pmatrix} 0 & 1.0000 & 0 & 0 \\ -1.0328 & 0 & 0 & 0.1439 \\ 0 & 0 & 0 & 1.0000 \\ 0.1884 & 0 & 0 & -0.0272 \end{pmatrix}$$

$$\mathbf{B}_7 = \begin{pmatrix} 0 \\ -0.1884 \\ 0 \\ 1.0328 \end{pmatrix}$$

$$\mathbf{A}_8 = \begin{pmatrix} 0 & 1.0000 & 0 & 0 \\ -1.0328 & 0 & 0 & -0.1439 \\ 0 & 0 & 0 & 1.0000 \\ 0.1884 & 0 & 0 & 0.0272 \end{pmatrix}$$

$$\mathbf{B}_8 = \begin{pmatrix} 0 \\ -0.1884 \\ 0 \\ 1.0328 \end{pmatrix}$$

$$\mathbf{A}_9 = \begin{pmatrix} 0 & 1.0000 & 0 & 0 \\ -1.0222 & 0 & 0 & -0.1578 \\ 0 & 0 & 0 & 1.0000 \\ 0.1572 & 0 & 0 & 0.0282 \end{pmatrix}$$

$$\mathbf{B}_9 = \begin{pmatrix} 0 \\ -0.1572 \\ 0 \\ 1.0222 \end{pmatrix}$$

$$\mathbf{A}_{10} = \begin{pmatrix} 0 & 1.0000 & 0 & 0 \\ -1.0222 & 0 & 0 & 0.1578 \\ 0 & 0 & 0 & 1.0000 \\ 0.1572 & 0 & 0 & -0.0282 \end{pmatrix}$$

$$\mathbf{B}_{10} = \begin{pmatrix} 0 \\ -0.1572 \\ 0 \\ 1.0222 \end{pmatrix}.$$

D. Derivation of Controllers and Simulation Results

This section derives controllers for the specifications by applying the polytopic model and the LMI theorems. Having the solution of the LMIs, the feedback gains are computed by (23), and the control value is computed by (8). In the present case, it is

$$u = -\left(\sum_{r=1}^{10} w_r(x_3, x_4)\mathbf{F}_r\right) x.$$

We compare the control results to various different alternative solutions [18], [21], [22]. An important difference from other controller design methods is that they are analytical solutions, while the present solution is automatically derived via numerical methods in a few minutes on a regular computer without analytical interaction. Further design specifications such as parameter uncertainty, robust control, etc., can be readily included in the design, if needed, by selecting other LMIs from the control literature. If the dynamic model is modified, then the design process can be repeated in a few minutes unlike the analytical solutions that may lead to hard work again, even in the case of a small modification.

1) Controller 1: We design here a controller that is capable of asymptotically stabilizing TORA and satisfying the above given constraints. We apply the following LMIs. The derivations and proofs of these theorems are fully detailed in [9].

Theorem 1 (Asymptotic Stability): The polytopic model (4) with control value (8) is asymptotically stable if there exist $\mathbf{X} > 0$ and $\mathbf{M}_r$ that satisfy

$$-\mathbf{X}\mathbf{A}_r^T - \mathbf{A}_r\mathbf{X} + \mathbf{M}_r^T\mathbf{B}_r^T + \mathbf{B}_r\mathbf{M}_r > \mathbf{0} \tag{21}$$

for all r and

$$-\mathbf{X}\mathbf{A}_r^T - \mathbf{A}_r\mathbf{X} - \mathbf{X}\mathbf{A}_s^T - \mathbf{A}_s\mathbf{X} + \mathbf{M}_s^T\mathbf{B}_r^T + \mathbf{B}_r\mathbf{M}_s + \mathbf{M}_r^T\mathbf{B}_s^T + \mathbf{B}_s\mathbf{M}_r \geq \mathbf{0} \tag{22}$$

for $r < s \leq R$, except the pairs (r, s) such that $w_r(\mathbf{p}(t))w_s(\mathbf{p}(t)) = 0$, $\forall \mathbf{p}(t)$, and where the feedback gains are determined from the solutions $\mathbf{X}$ and $\mathbf{M}_r$ as

$$\mathbf{F}_r = \mathbf{M}_r\mathbf{X}^{-1}. \tag{23}$$

In order to satisfy the constraints defined in Section III-C, the following LMIs are added to the previous ones.

Theorem 2 (Constraint on the Control Value): Assume that $\|\mathbf{x}(0)\| \leq \phi$, where $\mathbf{x}(0)$ is unknown, but the upper bound ϕ is known. The constraint $\|\mathbf{u}(t)\|_2 \leq \mu$ is enforced at all times $t \geq 0$ if the following LMIs hold:

$$\phi^2\mathbf{I} \leq \mathbf{X}$$
$$\begin{pmatrix} \mathbf{X} & \mathbf{M}_i^T \\ \mathbf{M}_i & \mu^2\mathbf{I} \end{pmatrix} \geq \mathbf{0}.$$

Theorem 3 (Constraint on the Output): Assume that $\|\mathbf{x}(0)\| \leq \phi$, where $\mathbf{x}(0)$ is unknown, but the upper bound ϕ is known. The constraint $\|\mathbf{y}(t)\|_2 \leq \lambda$ is enforced at all times $t \geq 0$ if the following LMIs hold:

$$\phi^2\mathbf{I} \leq \mathbf{X}$$
$$\begin{pmatrix} \mathbf{X} & \mathbf{X}\mathbf{C}_i^T \\ \mathbf{C}_i\mathbf{X} & \lambda^2\mathbf{I} \end{pmatrix} \geq \mathbf{0}.$$

The bounds of the control value and the output are guaranteed by Theorems 2 and 3. Thus, we solve these LMIs for the constrains together with the LMIs of Theorem 1 to guarantee asymptotic stability. By using the LMI solver of MATLAB Robust Control Toolbox, the following feasible solution and feedback gains are obtained for the controller:

$$\mathbf{X} = 10^8 \cdot \begin{pmatrix} 3.3742 & -0.1670 & -0.0002 & 2.1723 \\ -0.1670 & 3.4101 & -2.0928 & -0.2775 \\ -0.0002 & -2.0928 & 2.7746 & -0.5176 \\ 2.1723 & -0.2775 & -0.5176 & 1.8038 \end{pmatrix} > \mathbf{0}$$

$$\mathbf{F}_1 = (-2.1974 \;\; 0.6418 \;\; 1.5466 \;\; 3.6984)$$
$$\mathbf{F}_2 = (-2.1739 \;\; 0.6252 \;\; 1.5284 \;\; 3.6704)$$
$$\mathbf{F}_3 = (-2.2406 \;\; 0.5052 \;\; 1.4261 \;\; 3.5767)$$
$$\mathbf{F}_4 = (-1.6972 \;\; 0.1840 \;\; 1.0445 \;\; 2.8947)$$
$$\mathbf{F}_5 = (-1.6972 \;\; 0.1840 \;\; 1.0445 \;\; 2.8947)$$
$$\mathbf{F}_6 = (-2.2406 \;\; 0.5052 \;\; 1.4261 \;\; 3.5767)$$
$$\mathbf{F}_7 = (-2.3194 \;\; 0.6438 \;\; 1.5621 \;\; 3.7555)$$
$$\mathbf{F}_8 = (-1.7696 \;\; 0.3012 \;\; 1.1658 \;\; 3.0788)$$
$$\mathbf{F}_9 = (-1.2491 \;\; -0.0461 \;\; 0.7411 \;\; 2.2587)$$
$$\mathbf{F}_{10} = (-2.2971 \;\; 0.5544 \;\; 1.4757 \;\; 3.6503).$$

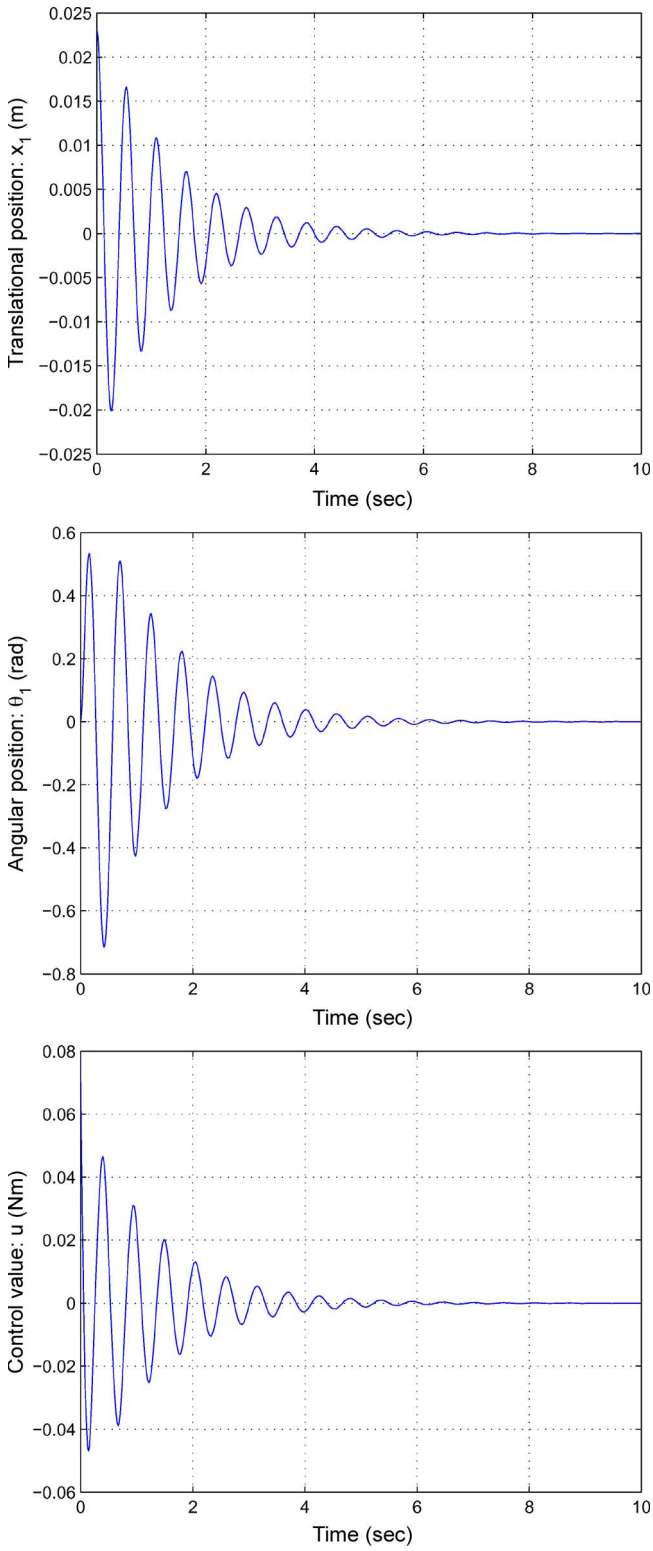

Fig. 5. Controller 1. Asymptotic stability control design with constraints, $x(0) = (0.023\ 0\ 0\ 0)$.

The simulation results, for the case of no trajectory, which are obtained using the `ode45` command of MATLAB Simulink, are depicted in Fig. 5 for the initial condition $x(0) = (0.023\ \text{m}\ \ 0\ \ 0\ \ 0)$.

If we compare this simulation to [22, Figs. 2 and 3, p. 394], which uses a measurement-schedules control method, or to

[21, Figs. 2 and 3], which discusses saturated passivity-based control results, we can generally conclude that these control results are very similar in the sense of settling time and the maximum of the control value. Both cited simulations used the same initial conditions that were used in our simulation.

The robustness of the controller is investigated through the performance for tracking a trajectory command whose shape was *a priori* unknown at the controller design phase. The simulation results are depicted in Fig. 6. The simulation shows that the controller is capable of tracking well the sinusoidal signal after 5 s but has difficulties with the linear oscillating signal.

2) Controller 2: In order to improve the tracking performance even for higher frequencies, we optimize the speed of the controller via decay rate control. The resulting controller offers a more aggressive control command for the actuator in order to maximize the speed of response, thus the tracking performance.

Theorem 4 (Decay Rate Control): Assume the polytopic model (4) with controller (8). The largest lower bound on the decay rate by quadratic Lyapunov function is guaranteed by the solution of the following generalized eigenvalue minimization problem:

$$\underset{X,M_1,\ldots,M_R}{\text{maximize}}\ \alpha \quad \text{subject to}$$

$$\mathbf{X} > \mathbf{0},$$

$$-\mathbf{X}\mathbf{A}_r^T - \mathbf{A}_r\mathbf{X} + \mathbf{M}_r^T\mathbf{B}_r^T + \mathbf{B}_r\mathbf{M}_r - 2\alpha\mathbf{X} > \mathbf{0},$$

$$-\mathbf{X}\mathbf{A}_r^T - \mathbf{A}_r\mathbf{X} - \mathbf{X}\mathbf{A}_s^T - \mathbf{A}_s\mathbf{X} + \mathbf{M}_s^T\mathbf{B}_r^T + \mathbf{B}_r\mathbf{M}_s + \mathbf{M}_r^T\mathbf{B}_s^T + \mathbf{B}_s\mathbf{M}_r - 4\alpha\mathbf{X} \geq \mathbf{0}$$

for $r < s \leq R$, except the pairs (r, s) such that $w_r(\mathbf{p}(t))w_s(\mathbf{p}(t)) = 0$, $\forall \mathbf{p}(t)$, and where the feedback gains are determined from the solutions by (23).

In order to set the constraints on the control input and the system output, we solve these LMIs together with the LMIs of Theorems 2 and 3, and the following feasible solution is obtained:

$$\mathbf{X} = 10^8 \cdot \begin{pmatrix} 0.6296 & -0.0943 & -0.0001 & 1.2269 \\ -0.0943 & 0.6990 & -1.1270 & -0.4600 \\ -0.0001 & -1.1270 & 5.0973 & -0.6500 \\ 1.2269 & -0.4600 & -0.6500 & 2.9933 \end{pmatrix} > \mathbf{0}$$

$$\mathbf{F}_1 = (-5.4952 \ \ 1.0838 \ \ 0.9800 \ \ 2.9270)$$
$$\mathbf{F}_2 = (-5.4382 \ \ 1.0358 \ \ 0.9648 \ \ 2.8935)$$
$$\mathbf{F}_3 = (-4.7511 \ \ 0.4630 \ \ 0.7955 \ \ 2.4494)$$
$$\mathbf{F}_4 = (-3.3691 \ \ -0.4181 \ \ 0.5147 \ \ 1.7323)$$
$$\mathbf{F}_5 = (-3.3691 \ \ -0.4181 \ \ 0.5147 \ \ 1.7323)$$
$$\mathbf{F}_6 = (-4.7511 \ \ 0.4630 \ \ 0.7955 \ \ 2.4494)$$
$$\mathbf{F}_7 = (-5.4584 \ \ 1.0358 \ \ 0.9701 \ \ 2.8844)$$
$$\mathbf{F}_8 = (-4.1158 \ \ 0.0830 \ \ 0.6675 \ \ 2.1627)$$
$$\mathbf{F}_9 = (-2.9451 \ \ -0.6436 \ \ 0.4369 \ \ 1.5402)$$
$$\mathbf{F}_{10} = (-5.0967 \ \ 0.7299 \ \ 0.8782 \ \ 2.6542).$$

The simulation results of Controller 2 for tracking the same trajectory command are depicted in Fig. 7. It can be observed that the decay rate controller has significantly better tracking performance and can also track well the linear oscillating signal after a short setup period, while Controller 1 has some difficulties. However, as expected, the decay rate controller achieves about twice as large maximum control value ($\max \|u\| = 0.102$ N · m compared to Controller 1, where $\max \|u\| = 0.062$ N · m) but still satisfies the control specification guaranteed by the LMI constraints.

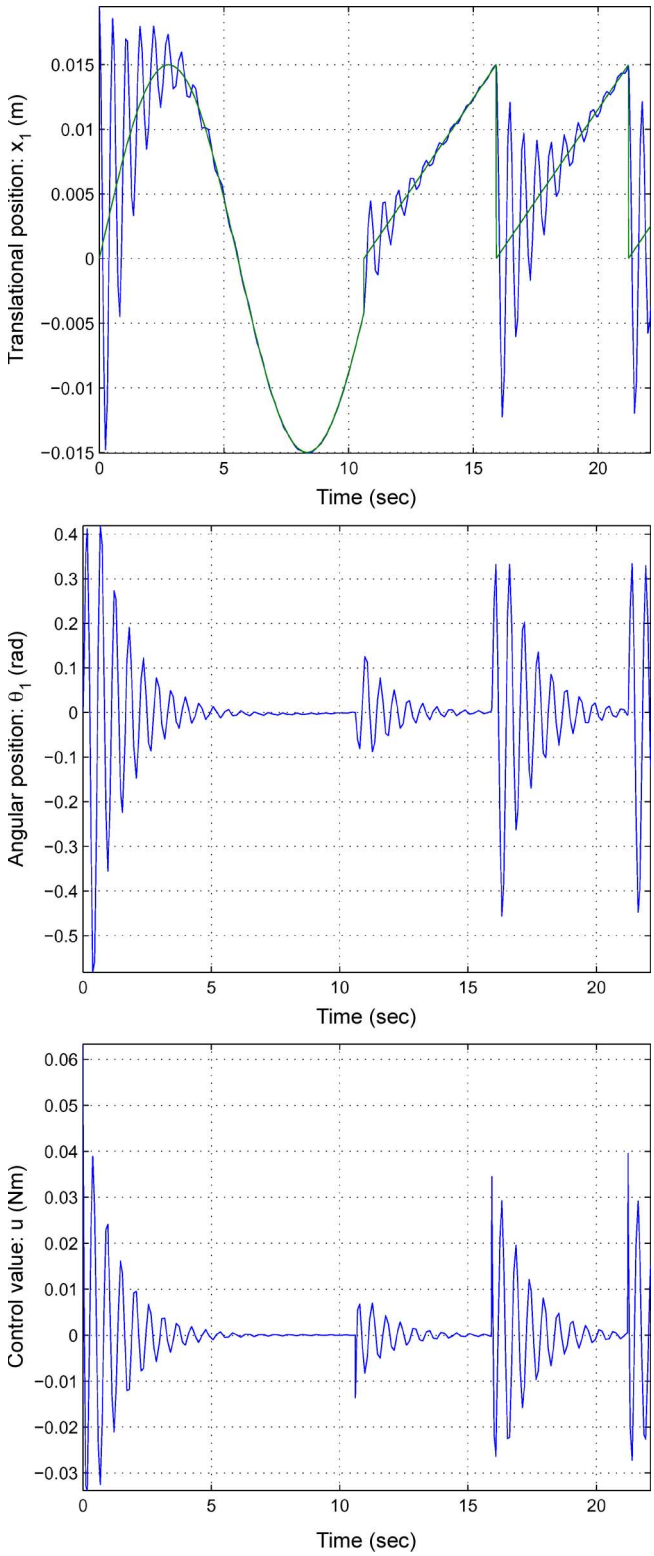

Fig. 6. Tracking by Controller 1.

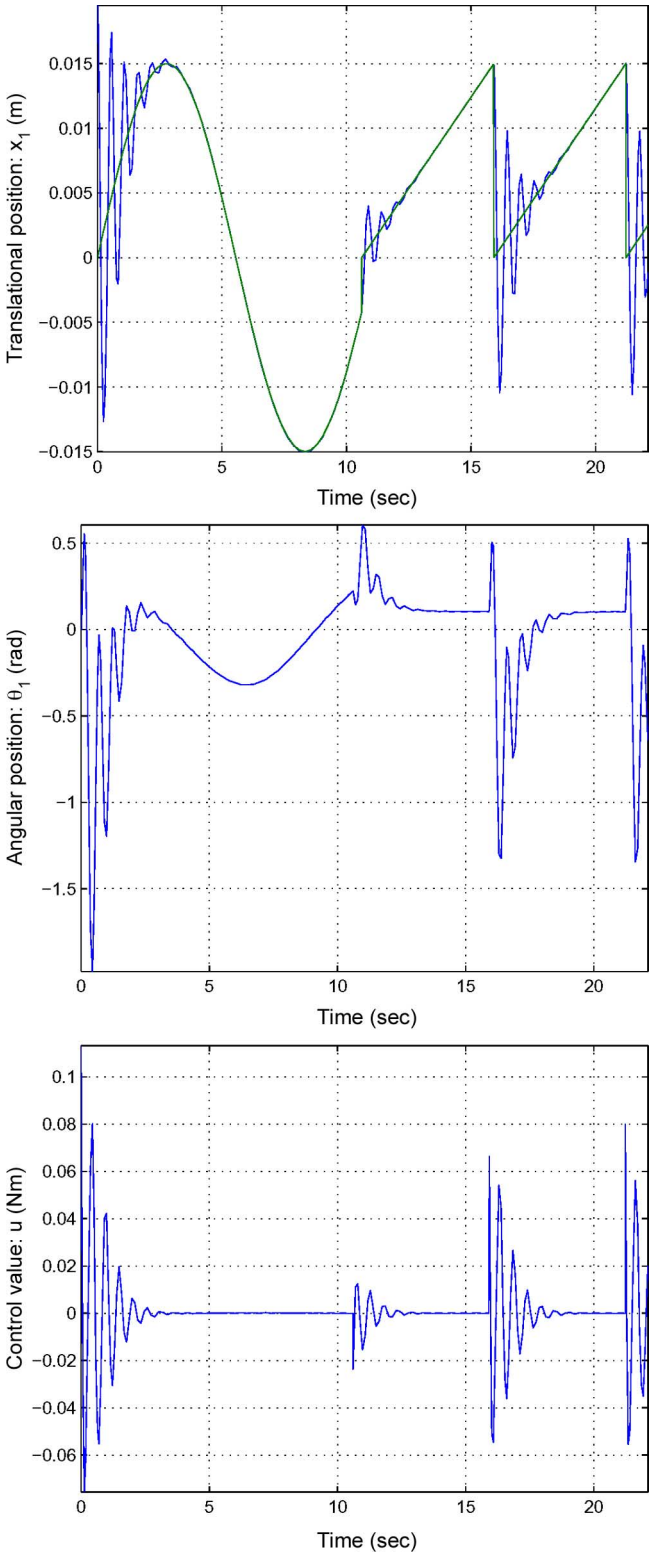

Fig. 7. Tracking by Controller 2 (decay rate controller).

IV. Conclusion

This paper has presented a study for trajectory tracking controller design of the TORA system using the TPDC framework. The TPDC controller design is shown to be an efficient and straightforward numerical controller design method to achieve the desired controller performance while the controller specification and constraints are guaranteed. This paper has given a trajectory tracking controller design example of the TORA system for general types of trajectory commands. The simulation proved that the decay rate controller significantly improved the tracking performance.

References

[1] S. Boyd, L. E. Ghaoui, E. Feron, and V. Balakrishnan, *Linear Matrix Inequalities in System and Control Theory*. Philadelphia, PA: SIAM, 1994.

[2] P. Gahinet, A. Nemirovski, A. J. Laub, and M. Chilali, *LMI Control Toolbox*. Natick, MA: The MathWorks, Inc., 1995.

[3] C. W. Scherer and S. Weiland, *Linear Matrix Inequalities in Control*, 2000. [Online]. Available: http://www.cs.ele.tue.nl/SWeiland/lmid.pdf

[4] K. Khayati, P. Bigras, and L.-A. Dessaint, "A multistage position/force control for constrained robotic systems with friction: Joint-space decomposition, linearization, and multiobjective observer/controller synthesis using lmi formalism," *IEEE Trans. Ind. Electron.*, vol. 53, no. 5, pp. 1698–1712, Oct. 2006.

[5] R. Amirifar and N. Sadati, "Low-order h_∞ controller design for an active suspension system via lmis," *IEEE Trans. Ind. Electron.*, vol. 53, no. 2, pp. 554–560, Apr. 2006.

[6] P. Baranyi and Y. Yam, "Case study of the tp-model transformation in the control of a complex dynamic model with structural nonlinearity," *IEEE Trans. Ind. Electron.*, vol. 53, no. 3, pp. 895–904, Jun. 2006.

[7] P. Baranyi, "TP model transformation as a way to LMI based controller design," *IEEE Trans. Ind. Electron.*, vol. 51, no. 2, pp. 387–400, Apr. 2004.

[8] P. Baranyi, D. Tikk, Y. Yam, and R. J. Patton, "From differential equations to PDC controller design via numerical transformation," *Comput. Ind.*, vol. 51, no. 3, pp. 281–297, Aug. 2003.

[9] K. Tanaka and H. O. Wang, *Fuzzy Control Systems Design and Analysis—A Linear Matrix Inequality Approach*. Hoboken, NJ: Wiley, 2001.

[10] P. Baranyi, "Tensor product model based control of 2-D aeroelastic system," *J. Guid. Control Dyn.*, vol. 29, no. 2, pp. 391–400, Mar./Apr. 2006.

[11] R. H. Rand, R. J. Kinesey, and D. L. Mingori, "Dynamics of spinup through resonance," *Int. J. Non-Linear Mech.*, vol. 27, no. 3, pp. 489–502, 1992.

[12] M. Jankovic, D. Fontanie, and P. V. Kokotovic, "Tora example: Cascade- and passivity-based control designs," *IEEE Trans. Control Syst. Technol.*, vol. 4, no. 3, pp. 292–297, May 1996.

[13] C. J. Wan, D. S. Bernstein, and V. T. Coppola, "Global stabilization of the oscillating eccentric rotor," *Nonlinear Dyn.*, vol. 10, no. 1, pp. 49–62, May 1996.

[14] R. Bupp, V. T. Coppola, and D. S. Bernstein, "Vibration suppression of multi-modal translational motion using a rotational actuator," in *Proc. IEEE Int. Decision and Control*, Orlando, FL, 1994, pp. 4030–4034.

[15] B. Wie and D. S. Bernstein, "Benchmark problems in robust control design," *J. Guid. Control Dyn.*, vol. 15, no. 5, pp. 1057–1059, 1992.

[16] R. Bupp, D. S. Bernstein, and V. T. Coppola, "A benchmark problem for nonlinear control design: Problem statement, experimental testbed, and passive nonlinear compensation," in *Proc. Amer. Control Conf.*, Seattle, WA, 1995, pp. 4363–4367.

[17] R. Bupp, D. S. Bernstein, and V. T. Coppola, "A benchmark problem for nonlinear control design," *Int. J. Robust Nonlinear Control*, vol. 8, no. 415, pp. 307–310, 1998.

[18] *Int. J. Robust Nonlinear Control (Special Issue on Control of the TORA System)*, vol. 8, pp. 305–457, 1998.

[19] G. Tadmor, "Dissipative design, lossless dynamics, and the nonlinear tora benchmark example," *IEEE Trans. Control Syst. Technol.*, vol. 9, no. 2, pp. 391–398, Mar. 2001.

[20] K. Tanaka, T. Taniguchi, and H. O. Wang, "Model based fuzzy control of TORA system: Fuzzy regulator and fuzzy observer design via LMIs that represent decay rate, disturbance rjection, robustness, optimality," in *Proc. Int. IEEE Conf. Fuzzy Syst.*, Anchorage, AK, 1998, pp. 313–318.

[21] G. Escobar, R. Ortega, and H. Sira-Ramirez, "Output-feedback global stabilization of a nonlinear benchmark system using a saturated passivity-based controller," *IEEE Trans. Control Syst. Technol.*, vol. 7, no. 2, pp. 289–293, Mar. 1999.

[22] S. Dussy and L. E. Ghaoui, "Measurement-scheduled control for the rtac problem: An lmi approach," *Int. J. Robust Nonlinear Control*, vol. 8, no. 4/5, pp. 377–400, 1998.

Zoltán Petres (S'03) was born in Hungary in 1980. He received the M.Sc. degree in computer science and information technology and the Ph.D. degree from Budapest University of Technology and Economics, Budapest, Hungary, in 2004 and 2007, respectively.

In 2004, he was a Huygens Scholarship Awarded Research Student in the Delft Center of Systems and Control, Delft University of Technology, Delft, The Netherlands. From October 2004 to March 2006, he was at Prof. Hashimoto's laboratory in the Institute of Industrial Science, The University of Tokyo, Tokyo, Japan. He is currently with the Computer and Automation Research Institute, Hungarian Academy of Sciences, Budapest. His research interests include nonlinear control techniques and cognitive vision.

Dr. Petres is a member of the Integrated Intelligent Systems Japanese–Hungarian Laboratory, the IFSA Hungarian Fuzzy Association, and the IEEE Industrial Electronics Society. He received the IFSA Hungarian Fuzzy Association Youth Award in 2004 and the Outstanding Paper Award at ISIS'05.

Péter Baranyi (M'00) was born in Hungary in 1970. He received the M.Sc. degree in electrical engineering, the M.Sc. degree in education of engineering sciences, and the Ph.D. degree from Budapest University of Technology and Economics, Budapest, Hungary, in 1994, 1995, and 1999, respectively. He received the D.Sc. degree from the Hungarian Academy of Sciences in 2006.

He has held research positions at The Chinese University of Hong Kong, Hong Kong, in 1996 and 1998, The University of New South Wales, Sydney, Australia, in 1997, the CNRS LAAS Institute, Toulouse, France, in 1996, the Gifu Research Institute, Gifu, Japan, in 2000–2001, and the University of Hull, Hull, U.K., in 2002–2003. He is currently with the Computer and Automation Research Institute, Hungarian Academy of Sciences, Budapest. His research interests include fuzzy and neural network techniques.

Dr. Baranyi is the Secretary General of the Hungarian Society of the International Fuzzy Systems Association. He was a founding member of the Integrated Intelligent Systems Japanese–Hungarian Laboratory. He received the Youth Prize of the Hungarian Academy of Sciences, the International Dennis Gábor Award in 2000, and the Outstanding Young Technological Innovator of the Year 2002-II Prize in Hungary.

Péter Korondi (M'98) received the Dipl. Eng. and Ph.D. degrees in electrical engineering from Technical University of Budapest, Budapest, Hungary, in 1984 and 1995, respectively.

Since 1986, he has been with Budapest University of Technology and Economics (formerly the Technical University of Budapest), Budapest. From April 1993 to April 1995, he was with Prof. Harashima and Prof. Hashimoto at the Institute of Industrial Science, The University of Tokyo, Tokyo, Japan, where he continues to spend a month each year working on joint research. As a result of this cooperation, the Intelligent Integrated System Japanese–Hungarian Joint Laboratory was founded in 2001. His research interests include telemanipulation and motion control.

Dr. Korondi is a founding member of the International PEMC Council, which became a chapter of the European Power Electronics Association.

Hideki Hashimoto (S'83–M'84–SM'04–F'06) received the B.Sc., M.Sc., and Dr. Eng. degrees in electrical engineering from The University of Tokyo, Tokyo, Japan, in 1981, 1984, and 1987, respectively.

From 1989 to 1990, he was a Visiting Scientist in the Laboratory for Informational and Decision Systems and the Laboratory for Electromagnetics and Electronics Systems, Massachusetts Institute of Technology, Cambridge. He is currently an Associate Professor in the Institute of Industrial Science, The University of Tokyo. His research interests are in the areas of robotics, control, intelligent transportation systems, and human–machine interface.

Dr. Hashimoto is an active member of the IEEE Industrial Electronics and IEEE Robotics and Automation Societies, and has served on the Administrative Committees of both. He is also a member of the Japanese Society of Instrument and Control Engineering, Institute of Electrical Engineers of Japan, and Robotics Society of Japan.